High Ca^{2+} permeability of a peptide-gated DEG/ENaC from *Hydra*

Stefan Dürrnagel,[1] Björn H. Falkenburger,[2] and Stefan Gründer[1]

[1]Department of Physiology and [2]Department of Neurology, RWTH Aachen University, 52074 Aachen, Germany

Degenerin/epithelial Na^+ channels (DEG/ENaCs) are Na^+ channels that are blocked by the diuretic amiloride. In general, they are impermeable for Ca^{2+} or have a very low permeability for Ca^{2+}. We describe here, however, that a DEG/ENaC from the cnidarian *Hydra magnipapillata*, the Hydra Na^+ channel (HyNaC), is highly permeable for Ca^{2+} (P_{Ca}/P_{Na} = 3.8). HyNaC is directly gated by *Hydra* neuropeptides, and in *Xenopus laevis* oocytes expressing HyNaCs, RFamides elicit currents with biphasic kinetics, with a fast transient component and a slower sustained component. Although it was previously reported that the sustained component is unselective for monovalent cations, the selectivity of the transient component had remained unknown. Here, we show that the transient current component arises from secondary activation of the Ca^{2+}-activated Cl^- channel (CaCC) of *Xenopus* oocytes. Inhibiting the activation of the CaCC leads to a simple on–off response of peptide-activated currents with no apparent desensitization. In addition, we identify a conserved ring of negative charges at the outer entrance of the HyNaC pore that is crucial for the high Ca^{2+} permeability, presumably by attracting divalent cations to the pore. At more positive membrane potentials, the binding of Ca^{2+} to the ring of negative charges increasingly blocks HyNaC currents. Thus, HyNaC is the first member of the DEG/ENaC gene family with a high Ca^{2+} permeability.

INTRODUCTION

Ion channels of the degenerin/epithelial Na^+ channel (DEG/ENaC) gene family are present in the genome of multicellular organisms ranging from sponges to humans. In unicellular organisms, genes with homology to DEG/ENaCs are absent, suggesting that DEG/ENaC ion channels have evolved in multicellular organisms, where they serve diverse functions (Kellenberger and Schild, 2002), ranging from mechanoreception in *Caenorhabditis elegans*, detection of salt and pheromones in *Drosophila melanogaster*, to neurotransmission and Na^+ reabsorption in mammals. Correspondingly, gating mechanisms of these channels are similarly diverse (Kellenberger and Schild, 2002) and range from direct mechanical gating to ligand gating, and some DEG/ENaCs are constitutively open. The diverse functions and gating mechanisms raise the question of the primordial function of these channels in the common ancestor of multicellular organisms. Which features are evolutionarily old and which are new?

Comparative analysis of DEG/ENaCs from evolutionarily separated groups of animals can help to answer this question. Animals of the phylum Cnidaria are among the most primitive multicellular animals. They are characterized by a radial symmetry and a primitive nervous system. Thus, the comparative analysis of DEG/ENaCs from cnidarians with those of other animals promises to yield important insights into the evolution of the DEG/ENaC gene family.

Hydra magnipapillata is an important model organism belonging to the class Hydrozoa within the phylum Cnidaria. Four cDNAs coding for DEG/ENaC subunits have been cloned from *Hydra* and the proteins named Hydra Na^+ channels (HyNaCs) (Golubovic et al., 2007; Dürrnagel et al., 2010); a fifth gene apparently encodes a pseudogene (Golubovic et al., 2007). HyNaC subunits 2, 3, and 5 assemble into a heteromeric channel, HyNaC2/3/5, which is directly gated by neuropeptides of the *Hydra* nervous system (Dürrnagel et al., 2010), Hydra-RFamides I and II (pQWLGGRF-NH_2 and pQWFNGRF-NH_2, respectively) (Moosler et al., 1996). Because peptide-gated DEG/ENaCs also exist in mollusks (Cottrell et al., 1990; Lingueglia et al., 1995), and because H^+-gated acid-sensing ion channels (ASICs) from chordates are closely related to HyNaCs (Golubovic et al., 2007), the common ancestor of DEG/ENaCs from Cnidaria and bilateral organisms was probably a channel gated by an extracellular ligand, perhaps a peptide.

In contrast to their diverse functions and gating mechanisms, all DEG/ENaCs share a secondary structure with two transmembrane domains and a large extracellular domain (Kellenberger and Schild, 2002). Moreover, most DEG/ENaCs share two biophysical characteristics: they are Na^+ selective, and they are blocked by the diuretic amiloride.

Correspondence to Stefan Gründer: sgruender@ukaachen.de

Abbreviations used in this paper: ASIC, acid-sensing ion channel; $[Ca^{2+}]_i$, intracellular Ca^{2+} concentration; CaCC, Ca^{2+}-activated Cl^- channel; DEG/ENaC, degenerin/epithelial Na^+ channel; E_{rev}, reversal potential; HyNaC, Hydra Na^+ channel; NPPB, 5-nitro-2-(3-phenylpropylamino)-benzoate; wt, wild type.

The Rockefeller University Press $30.00
J. Gen. Physiol. Vol. 140 No. 4 391–402
www.jgp.org/cgi/doi/10.1085/jgp.201210798

Some ASICs are an exception to this rule because at prolonged activation, their selectivity changes from Na^+ selective to unselective for monovalent cations. This happens at physiological ligand concentrations for shark ASIC1b (Springauf and Gründer, 2010) and at high ligand concentrations (low pH) for ASIC3 (Lingueglia et al., 1997). The Na^+-selective state typically is associated with rapidly activating and desensitizing peak currents, whereas the unselective state is associated with small sustained currents. Thus, some ASICs apparently have a dynamic selectivity. When expressed in *Xenopus laevis* oocytes, HyNaC currents resemble the biphasic ASIC currents: a fast transient current is followed by a comparatively large sustained current, and the sustained current is indeed a relatively unselective current (Golubovic et al., 2007; Dürrnagel et al., 2010).

Here, we show that the transient peptide-activated current is not a Na^+ current but rather arises from secondary activation of the Ca^{2+}-activated Cl^- channel (CaCC) that is endogenous to *Xenopus* oocytes (Miledi, 1982; Barish, 1983; Schroeder et al., 2008). Inhibiting activation of the CaCC abolishes transient currents and leads to simple on–off responses of HyNaC without any apparent desensitization. Collectively, our results show that the kinetics of HyNaC currents is simple and that the HyNaC pore is cation unselective with a high Ca^{2+} permeability (P_{Ca}/P_{Na} = 3.8). These results suggest that primordial DEG/ENaCs may have been unselective cation channels and that a highly Na^+-selective pore may be an advanced feature of channels from this gene family.

MATERIALS AND METHODS

Electrophysiology

cDNAs for HyNaCs 2, 3, and 5 had been described (Golubovic et al., 2007; Dürrnagel et al., 2010), and mutants of the Ca^{2+}-binding site were constructed as described previously (Paukert et al., 2004). Mutants of the Ca^{2+}-binding site replaced a conserved aspartate residue by a cysteine (D431C in HyNaC2, D433C in HyNaC3, and D438C in HyNaC5). Capped cRNA was synthesized by SP6 RNA polymerase from linearized cDNA using the mMessage mMachine kit (Ambion). Hydra-RFamide I (pQWLGGRF-NH_2) was purchased from Genemed Synthesis.

For expression of HyNaC2/3/5, ∼0.8 ng cRNA was injected into defolliculated stage V–VI oocytes of *Xenopus* and oocytes were kept in oocyte Ringer's solution 2 (OR-2) 2–4 d before measurements; for expression of HyNaC2/3/5_D-C and P2X4, ∼16 ng cRNA was injected. OR-2 contained (in mM): 82.5 NaCl, 2.5 KCl, 1.0 Na_2HPO_4, 1.0 $MgCl_2$, 1.0 $CaCl_2$, 5.0 HEPES, 0.5 g/liter PVP, 1,000 U/l penicillin, and 10 mg/l streptomycin, with pH adjusted to 7.3 with NaOH. Whole cell currents were recorded with an amplifier (TurboTec 03X; npi electronic), using an automated pump-driven solution exchange system together with the oocyte-testing carousel controlled by the interface OTC-20 (Madeja et al., 1995). Data acquisition and solution exchange were managed using the software CellWorks (version 5.1.1; npi electronic). Data were filtered at 20 Hz and acquired at 0.1–1 kHz.

Standard bath solution for whole oocyte current measurements contained (in mM): 140 NaCl, 10 HEPES, 1.8 $CaCl_2$, and 1.0 $MgCl_2$, with pH 7.4 adjusted with NaOH. To avoid activation of CaCCs, we injected 50 nl of either EGTA solution (in mM: 20 EGTA and 10 HEPES, pH 7.4) or BAPTA solution (in mM: 20 BAPTA and 10 HEPES, pH 7.4) into oocytes, 15–120 min before recordings. Glass electrodes filled with 3 M KCl were used; they had a resistance of 0.3–1.5 MΩ. If not specified, the membrane potential was clamped at −70 mV.

Photometric calcium measurements

Oocytes were injected with 50 nl Fura-2AM (1 mM) 30–120 min before the recording (the AM ester form was used solely because of availability) and placed with the animal pole facing away from the objective. Measurements used a BX51WI upright microscope (Olympus) with a 40× water-immersion objective (NA 0.8) and a TILL photometry system (TILL Photonics). The region of interest chosen for recording included most of the upper surface of the cell. We do not know how far into the oocyte our optics penetrate but do not expect it to be more than a few micrometers. Fura-2 was excited every 2 s with a 100-ms pulse of 340 nm light and a 50-ms pulse of 380 nm light using a Polychrome 5 light source (TILL Photonics). Emission was collected by a photodiode (TILL Photonics) behind a 535/30-nm bandpass filter, digitized at 5 kHz by a LIH8+8 interface run by Patchmaster software (HEKA). Emission during the 340-nm pulse and the 380-nm pulse was averaged, and the F340/F380 ratio was determined for each time point (emission with 340-nm excitation/emission with 380-nm excitation). Because emission was generally lower with 340-nm than with 380-nm excitation, a longer recording was taken for the 340-nm excitation to increase the signal-to-noise ratio. Simultaneously, currents were recorded with the TurboTec 03X amplifier and digitized at 0.1 kHz using the LIH8+8 interface. To activate HyNaCs, 500 µl Hydra-RFamide I (10 µM) was manually applied to the Petri dish to achieve a final concentration of ∼1 µM. Data were analyzed offline using IGOR (WaveMetrics). The changes induced by HyNaC agonists were reproducible and large compared with the signal-to-noise ratio (see Fig. 5 A). On average, they were 47 ± 9% of the baseline F340/F380 ratio and small compared with the variation between cells in the resting F340/F480 ratio (see Fig. 5 B). We therefore did not aim to calibrate the F340/F380 signal and to convert the obtained numbers into absolute concentrations of Ca^{2+}.

Data analysis

For determination of reversal potentials (E_{rev}s) and calculation of relative permeabilities, oocytes were injected with 20 mM EGTA to minimize the influence of CaCCs. All I-V relationships were corrected for background conductances by subtracting the currents measured at a given voltage without agonist application.

Ionic permeability ratio for monovalent cations P_{Na}/P_K was calculated from the shift in E_{rev} when NaCl in the standard bath solution was replaced by an equimolar amount of KCl, according to the following equation derived from the Goldman–Hodgkin–Katz equation:

$$\frac{P_{Na}}{P_K} = \frac{\left[K^+\right]_o}{\left[Na^+\right]_o} e^{\left(\frac{\Delta E_{rev} * F}{R * T}\right)}, \quad (1)$$

where $\Delta E_{rev} = E_{Na} - E_K$, R is the gas constant, F the Faraday constant, and T the temperature. We assumed that the intracellular concentrations of Na^+ and K^+ are constant within one batch of oocytes.

Assuming additionally that intracellular Ca^{2+} concentration ($[Ca^{2+}]_i$) is very small, P_{Ca}/P_{Na} can be calculated from the shift in E_{rev} when Na^+ was replaced by Ca^{2+} in the application solution, according to the following equation (Lewis, 1979; Bässler et al., 2001):

$$\frac{P_{Ca}}{P_{Na}} = \frac{\left[Na^+\right]_o \left(1 + e^{\frac{E_{Ca} * F}{R * T}}\right)}{4\left[Ca^{2+}\right]_o \; e^{\frac{\Delta E_{REV} * F}{R * T}}}, \quad (2)$$

where $\Delta E_{rev} = E_{Na} - E_{Ca}$, and R, T, and F have the same meaning as above. The solution used to determine E_{Ca} contained (in mM): 10 $CaCl_2$, 126.5 NMDG-Cl, and 10 HEPES, pH 7.4. The solution used to determine E_{Na} contained (in mM): 140 NaCl, 1 $CaCl_2$, and 10 HEPES, pH 7.4; the minor amount of Ca^{2+} in this solution was considered negligible.

Activity of ions was used in all terms of $[c]$. Activity coefficients f_i of single ions i of valence z were calculated for Na^+ and Ca^{2+} with the Davies equation (Davies, 1962):

$$\log_{10} f_i = -0.509 z^2 \left(\frac{\sqrt{I}}{1 + \sqrt{I}} - 0.2\, I \right), \quad (3)$$

where I is the ionic strength, which is defined as:

$$I = 0.5 \sum c_i z_i^2. \quad (4)$$

In all figures showing voltage ramps (Figs. 1 C, 4, 6, and 7, D, F, and G), the individual conditions were measured with different oocytes of the same batch (except measurements for the P_2X_4 receptor, which were performed on separate batches). Furthermore, batches of oocytes were identical between Figs. 4 and 7 D and between Figs. 6 A and 7 F. The use of separate oocytes was necessary, as leak currents usually increased over time, especially when oocytes were clamped at holding potentials more negative than −70 mV.

Results are expressed as mean ± SEM. Statistical significance was determined using Student's paired or unpaired *t* test, as appropriate.

RESULTS

The transient current in HyNaC-expressing oocytes is carried by Cl^-

Fig. 1 A illustrates the typical biphasic currents elicited by Hydra-RFamide I (Moosler et al., 1996) in oocytes expressing HyNaC2/3/5 (named HyNaC in the remainder of this study, for simplicity). A fast transient current was followed by a slower sustained current; the ratio of transient and sustained currents was variable. Typically, a second peptide application elicited a similar response but of smaller amplitude (72 ± 8% of the first amplitude; $n = 11$; $P < 0.01$; Figs. 1 A and 2 A, bottom). A third application elicited a response of similar amplitude as the second (74 ± 9% of the first amplitude; $n = 11$; $P < 0.01$; Figs. 1 A and 2 A, bottom). The basis for this inactivation between the first and second application has remained unclear.

Previously, we determined E_{rev}s of the sustained current by stepping to different voltages during long agonist applications (Dürrnagel et al., 2010); E_{rev} was around +10 mV, indicating a relatively unselective cation current. Now, we determined E_{rev} of the peptide-activated currents by repeatedly activating HyNaC at different holding potentials between −70 and +20 mV and noticed that transient and sustained components had different E_{rev}s (Fig. 1, B and C). Although at −20 mV the transient current was clearly outward, the sustained current was inward, showing that both currents had different ion selectivity. Although the strong rectification rendered a precise determination of E_{rev} of the sustained current difficult, we estimated it to be 2 ± 3 mV ($n = 6$; Fig. 1 C), similar to what had been reported previously (Dürrnagel et al., 2010). In contrast, E_{rev} of the transient current was −22 ± 2 mV ($n = 6$; Fig. 1 C). Thus, the transient current clearly had different ion selectivity than the sustained current ($P < 0.001$). The leftward shift of the E_{rev}, however, was not compatible with an increased Na^+ selectivity of the transient current. In addition, it is notable that at more depolarized potentials, the amplitude of the transient outward current decreased rather than increased in amplitude (Fig. 1, B and C).

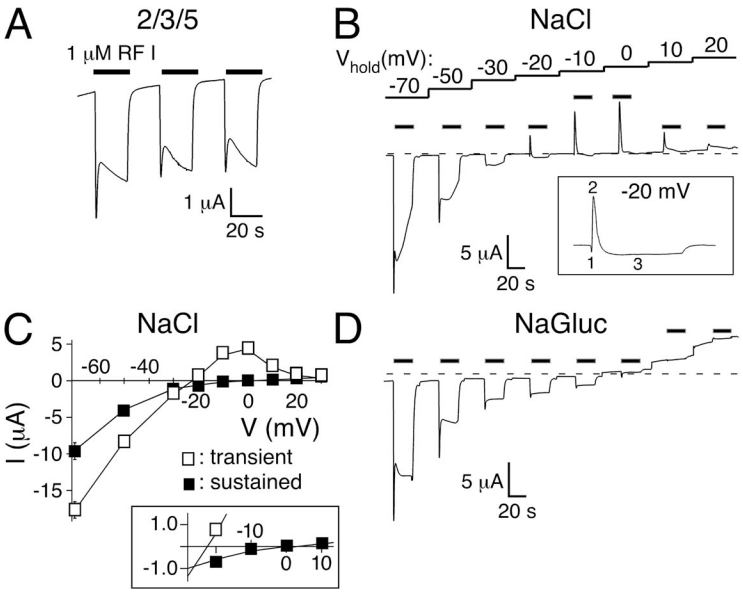

Figure 1. Transient peptide-activated currents depend on Cl^-. (A) Representative current trace showing activation of HyNaC2/3/5 in standard bath. HyNaC was activated with 1 µM Hydra-RFamide I (black bars). (B) Repeated activation of HyNaC at different holding potentials (V_{hold}) reveals the different E_{rev}s of the transient and the sustained current component. A representative current trace in standard bath solution is shown. Note that the transient current changes to outward at more negative potentials than the sustained current. The inset highlights the three current phases (initial inward, transient outward, and sustained inward) at a holding potential of −20 mV. (C) I/V plot revealing the different E_{rev}s of the transient (open squares) and sustained current components (closed squares) in standard bath ($n = 6$). Note the strong inward rectification of both components. The inset shows the I/V relations close to the E_{rev}s on an expanded scale. (D) Representative current trace in bath solution lacking Cl^- (NaCl replaced by NaGluconate). Note the absence of transient outward currents.

This decreased amplitude can now be attributed to a block by Ca^{2+} that inhibits flux of ions at more depolarized potentials (see below).

Assuming an intracellular Cl^- concentration of 33 mM, as reported for immature oocytes (Barish, 1983), in our solutions the Cl^- equilibrium potential was −38 mV, close to E_{rev} of the transient current. We therefore explored whether Cl^- contributed to the transient current and determined E_{rev} in Cl^--free solutions. Under these conditions, outward currents caused by influx of Cl^- were abolished (Fig. 1 D). Although E_{rev} of the sustained current was not changed (E_{rev} = 0.6 ± 2.8 mV; n = 5; P = 0.8), no transient outward currents were observed, strongly suggesting that the transient outward current in Cl^--containing solutions was carried by Cl^-.

Xenopus oocytes contain a CaCC in their plasma membrane, which is activated by increases in $[Ca^{2+}]_i$ (Miledi, 1982; Barish, 1983). Activation of the CaCC leads to biphasic currents: an initial transient Cl^- current (Miledi, 1982; Barish, 1983; White and Aylwin, 1990) is followed by sustained Cl^- currents (Boton et al., 1990; Wu and Hamill, 1992; Schroeder et al., 2008), resembling the appearance of peptide-activated currents in HyNaC-expressing oocytes. Moreover, repeated activation of the CaCC leads to reduced responses (Boton et al., 1990; Wu and Hamill, 1992) akin to the reduced amplitude of peptide-activated currents with repeated peptide application (Figs. 1 A and 2 A, bottom). We therefore considered that HyNaC is permeable to Ca^{2+} and that HyNaC activated the CaCC of oocytes. Closer inspection of measurements at a holding potential slightly positive to the Cl^- equilibrium potential (−20 mV) indeed revealed a current with three phases (Fig. 1 B, inset): an initial inward current, which could reflect an initial influx of cations through HyNaCs, was followed by a transient outward current, presumably carried by the influx of Cl^-, and a third sustained inward current, again dominated by influx of cations through HyNaCs.

The transient current is mediated by the endogenous CaCC

To test for the activation of the CaCC, we injected oocytes with either EGTA or BAPTA to chelate Ca^{2+} and prevent a rise in intracellular $[Ca^{2+}]$ and activation of the CaCC. Under these conditions, transient currents were indeed completely abolished, and peptide-activated currents had a step-like appearance with no strong desensitization (Fig. 2 A). Moreover, a second peptide application elicited a current of similar amplitude as the first application (for EGTA: 96 ± 5% of the first amplitude, P = 0.7; for BAPTA: 94 ± 2% of the first amplitude, P < 0.01; paired t test; n = 11; Fig. 2 A). In addition to the disappearance of transient currents, sustained currents had significantly smaller amplitudes after injection of EGTA or BAPTA (for EGTA: 43 ± 6% of the sustained current amplitude without EGTA injection, P < 0.01; for BAPTA: 47 ± 6% of the sustained current amplitude without BAPTA injection, P < 0.01; n = 11; Fig. 2 A), suggesting that the CaCC current may contribute not only to the transient but also to the sustained component of the peptide-activated currents. There were no significant differences in oocytes injected with EGTA or BAPTA. Therefore, in the remainder of this study, we used EGTA to prevent a rise in intracellular $[Ca^{2+}]$.

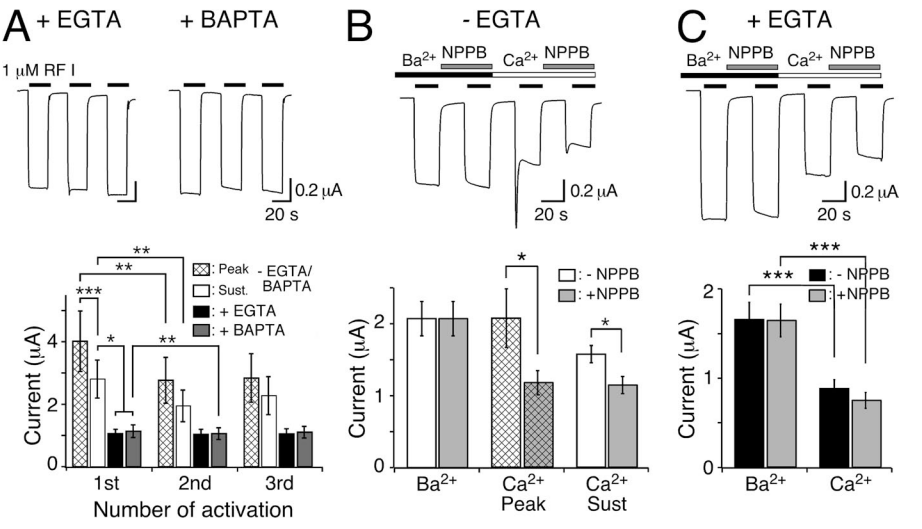

Figure 2. Chelation of $[Ca^{2+}]_i$ abolishes transient peptide-activated currents. (A; top) Representative HyNaC2/3/5 currents in oocytes injected with EGTA or BAPTA. Note the absence of a transient current and the step-like appearance of the currents. (Bottom) Bar graphs comparing the peak (hatched bars) and sustained (open bars) current amplitudes of oocytes expressing HyNaC and of oocytes expressing HyNaC and injected with EGTA (closed bars) or BAPTA (gray bars) (n = 11). (B; top) Representative current trace comparing peptide-activated currents in standard bath and in standard bath in which $CaCl_2$ was replaced by an equimolar amount (1.8 mM) of $BaCl_2$. Currents were measured either in the presence or the absence of 100 μM NPPB. Oocytes were preincubated for 20 s in the corresponding test solutions before activation by 1 μM RFamide I. (Bottom) Bar graph comparing the current amplitudes in the absence of NPPB (open bars) and in the presence of 100 μM NPPB (gray bars) for the indicated conditions. In the presence of Ba^{2+}, no transient current was discernible. The application sequence of the individual solutions was shuffled (n = 8). (C) As in B, for oocytes that had been injected with EGTA. Note the absence of peak currents. (Bottom) Bar graph comparing the current amplitudes in the absence of NPPB (closed bars) and in the presence of 100 μM NPPB (gray bars) for sustained currents. *, P < 0.05; **, P < 0.01; ***, P < 0.001.

To further test for the activation of the CaCC, we replaced extracellular Ca^{2+} by Ba^{2+}, which does not activate CaCCs (Barish, 1983). Indeed, in the presence of Ba^{2+}, peptide-activated currents had a step-like appearance like after chelation of intracellular Ca^{2+} (Fig. 2 B). Furthermore, we pharmacologically blocked CaCC by 5-nitro-2-(3-phenylpropylamino)-benzoate (NPPB) (Wu and Hamill, 1992). 100 µM NPPB reduced the amplitude of transient currents by about half and of sustained currents by 28% ($P < 0.05$; $n = 8$; Fig. 2 B), indicating partial block of CaCCs by 100 µM NPPB, which is similar to previous reports (Wu and Hamill, 1992; Schroeder et al., 2008).

We wanted to exclude that NPPB had a direct effect on HyNaC and repeated those experiments with EGTA-injected oocytes. The amplitudes of currents in the presence of Ba^{2+} were now approximately twofold increased compared with currents in the presence of Ca^{2+} ($n = 8$; $P < 0.001$), suggesting either that Ba^{2+} potentiated HyNaC currents or that Ca^{2+} blocked them. NPPB slightly reduced the amplitude of HyNaC currents from 0.88 ± 0.1 to 0.75 ± 0.09 µA ($n = 8$; $P = 0.2$; paired t test; Fig. 2 C), indicating that NPPB has no strong direct effect on HyNaC.

Our results so far strongly argue for an activation of the endogenous CaCC by HyNaCs. Peptide-activated inward currents of HyNaC-expressing oocytes apparently are the sum of a Na^+ current flowing through HyNaCs and a Cl^- current flowing through CaCCs, with CaCCs being responsible for the biphasic kinetics of the currents. We directly tested this interpretation by activating HyNaCs in the absence of extracellular Na^+ (Fig. 3 A). We replaced all Na^+ by the large monovalent cation $NMDG^+$ (but kept 1 mM Ca^{2+}), which should abolish most of HyNaC inward currents. Under these conditions, Hydra-RFamide I still elicited a current with biphasic kinetics but of smaller amplitude. Peak current amplitudes were ∼70% ($n = 4$; $P = 0.14$) and sustained currents ∼30% ($n = 4$; $P < 0.001$) of the currents measured in standard NaCl solution. In control experiments with a solution containing $NMDG^+$ nominally free of Ca^{2+}, no inward current was observed ($n = 4$; Fig. 3 A). These results are consistent with the idea that Ca^{2+} influx through HyNaCs secondarily activated CaCCs, greatly amplifying the HyNaC current.

To directly show Ca^{2+} influx through HyNaC, we activated HyNaC in the presence of 10 mM Ca^{2+} as the exclusive extracellular cation and in EGTA-injected oocytes to prevent activation of the CaCC (Fig. 3 B). Under these conditions, Hydra-RFamide I indeed induced a step-like inward current with an amplitude of 0.15 ± 0.01 µA ($n = 11$; Fig. 3 B), directly demonstrating robust influx of Ca^{2+} through HyNaC. The addition of an equimolar concentration of Na^+ (10 mM) only slightly increased the current amplitude to 0.16 ± 0.01 µA ($n = 11$; $P < 0.01$), whereas in the presence of 10 mM Na^+ as the exclusive cation, peptide-activated currents were increased approximately threefold (0.47 ± 0.04 µA; $n = 11$; $P < 0.001$; Fig. 3 B). The smaller current amplitude with a higher total concentration of permeant cations (10 mM Ca^{2+}/10 mM Na^+ compared with 10 mM Na^+ alone) suggests that Ca^{2+} blocks HyNaC in addition to permeating it. This behavior as a permeant blocker prohibits a direct quantitative comparison of the inward Na^+ and Ca^{2+} currents.

HyNaCs are unselective cation channels

Previously, we determined an E_{rev} of sustained peptide-activated currents in HyNaC-expressing oocytes of ∼10 mV and concluded that HyNaCs are unselective cation channels (Golubovic et al., 2007; Dürrnagel et al., 2010). We now show that sustained peptide-activated currents are contaminated by Cl^- currents through CaCCs, requiring reevaluation of E_{rev} of HyNaCs. We activated HyNaCs in oocytes for 50 s and stepped the holding potential from −70 to +30 mV in steps of 10 mV every 5 s. We determined E_{rev} in three different solutions: (1) standard bath, (2) standard bath with EGTA-injected oocytes, and (3) standard bath in which Ca^{2+} had been replaced by Ba^{2+} (Fig. 4). Like reported previously (Dürrnagel et al., 2010) and as already shown in Fig. 1 B,

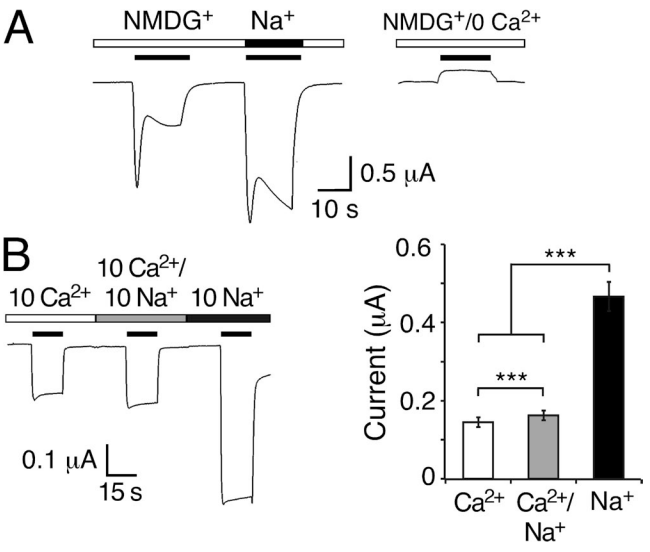

Figure 3. Peptide-activated currents in the absence of Na^+_e. (A; left) Representative current trace for HyNaC2/3/5 in solutions containing 1 mM Ca^{2+} together with 140 mM of either $NMDG^+$ or Na^+. 1 µM RFamide I was used for activation. (Right) Control experiment in $NMDG^+$ solution nominally free of Ca^{2+}. Similar results were observed in four out of four oocytes. (B; left) Representative current trace for HyNaC2/3/5 in solutions containing 10 mM Ca^{2+}, 10 mM Ca^{2+} and 10 mM Na^+, or 10 mM Na^+ (nominally free of Ca^{2+}). Solutions additionally contained 10 mM HEPES, pH 7.4, and $NMDG^+$ at concentrations to reach similar osmolarity (10 Ca^{2+}: 125 mM NMDGCl; 10 Ca^{2+}/10 Na^+: 115 mM NMDGCl; and 10 Na^+: 130 mM NMDGCl). Oocytes had been injected with EGTA; 2 µM RFamide I was used for activation. Holding potential was −85 mV. (Right) Quantitative comparison of current amplitudes. ***, $P < 0.001$.

in standard bath, currents had an E_{rev} of 11.5 ± 2.5 mV (n = 8) and were characterized by strong inward rectification. In EGTA-injected oocytes, E_{rev} was shifted to more positive values (24.0 ± 3.7 mV; n = 6; P < 0.05) and currents were also inwardly rectifying. It should be noted that the strong inward rectification in these two conditions rendered the determination of E_{rev} imprecise. When we replaced Ca^{2+} by Ba^{2+}, two things changed: E_{rev} was shifted to 3.0 ± 1.9 mV (n = 7; P < 0.05), and I-V relations became linear. These results show, first, that HyNaCs indeed have an E_{rev} indicative of a relatively unselective cation channel and, second, that extracellular Ca^{2+} is the cause of their inward rectification, presumably by blocking HyNaCs at more positive voltages. This Ca^{2+} block could explain why currents were enhanced when Ca^{2+} was replaced by Ba^{2+} (Fig. 2 C), why transient Cl^- currents were smaller at more depolarized potentials in standard bath (Fig. 1 B), and why Na^+ currents were strongly reduced by an equimolar amount of Ca^{2+} (Fig. 3 B). We conclude that Ca^{2+} is a permeant blocker of HyNaCs and that the block is voltage dependent. Ca^{2+} strongly blocks HyNaC already at −85 mV (Fig. 3 B) but more strongly as the membrane potential becomes more depolarized, leading to an almost complete block of HyNaC at positive potentials (Fig. 4). At present, we do not have a definite explanation for the shift of E_{rev} when Ca^{2+} had been replaced by Ba^{2+} (Fig. 4).

Ca^{2+} permeability of HyNaC is high

Activation of CaCCs indirectly measures Ca^{2+} permeation through HyNaC. To directly measure Ca^{2+} permeation, we additionally performed photometric Ca^{2+} measurements using Fura-2. The application of Hydra-RFamide I to oocytes that expressed HyNaC and had been injected with Fura-2 led to a robust increase in the F340/F380 ratio, indicating an increase in cytosolic Ca^{2+} (Fig. 5 A). Simultaneous measurement of currents revealed that the $[Ca^{2+}]_i$ increase paralleled the opening of the HyNaC pore (Fig. 5 A). $[Ca^{2+}]_i$ quickly rose after channel opening and remained high during channel activation. A similar rise in $[Ca^{2+}]_i$ was observed in all oocytes tested (n = 8; P < 0.001; paired t test; Fig. 5 B). The robust signal in photometric Ca^{2+} measurements after the opening of HyNaCs and the robust activation of CaCCs by HyNaC suggest a high Ca^{2+} permeability of HyNaCs.

We then estimated the relative Ca^{2+} permeability of HyNaC by determining E_{rev} in two different Ca^{2+} concentrations and with EGTA-injected oocytes. To increase the contribution of the Ca^{2+} current to the total current, we replaced Na^+ by the larger impermeant cation $NMDG^+$. In 1 mM Ca^{2+}, E_{rev} was −43 ± 1.5 mV (n = 9), whereas in 10 mM Ca^{2+}, it was significantly shifted to −17 ± 2.6 mV (n = 10; P < 0.001; Fig. 6 A). To assess these values, we made identical measurements with P2X4, a purinergic ion channel of known high Ca^{2+} permeability (P_{Ca}/P_{mono} = 4.2; Soto et al., 1996). In fact, E_{rev} of P2X4 in 1 and 10 mM Ca^{2+} was similar to previously published values for P2X4 (Soto et al., 1996) and to E_{rev} of HyNaC (Fig. 6 B), suggesting that P_{Ca}/P_{mono} of HyNaC is on the same order as that of P2X4.

Finally, we calculated the relative Ca^{2+} permeability P_{Ca}/P_{Na} of HyNaC by determining the shift in E_{rev} when the solution contained either Ca^{2+} or Na^+ as the main permeant cation. As mentioned above, E_{rev} with 10 mM Ca^{2+} was −17 ± 2.6 mV and with 140 mM Na^+ it was

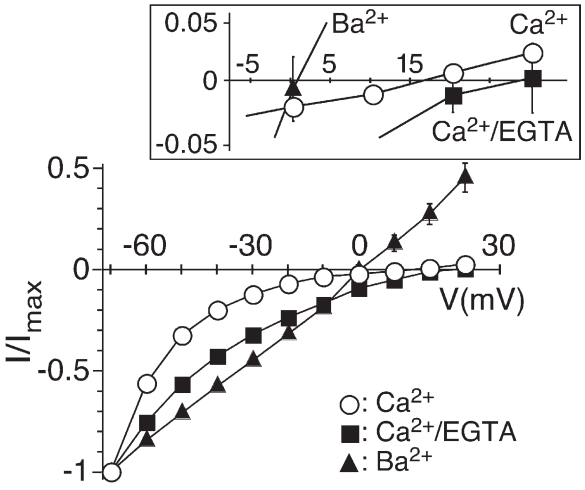

Figure 4. Preventing a rise in $[Ca^{2+}]_i$ changes E_{rev} of sustained peptide-activated currents. I/V relations for HyNaC2/3/5 activated by 1 µM Hydra-RFamide I in standard bath (open circles), in standard bath after injection of EGTA (closed squares), and in standard bath in which $CaCl_2$ had been replaced by $BaCl_2$ (closed triangles). Currents were normalized to the current measured at −70 mV, which had an amplitude of −4.4 ± 1.1 µA (Ca^{2+}), −1.4 ± 0.2 µA (Ca^{2+}/EGTA), or −6.0 ± 0.8 µA (Ba^{2+}) (n = 7 - 8), respectively. The inset shows the I/V relations close to the E_{rev}s on an expanded scale.

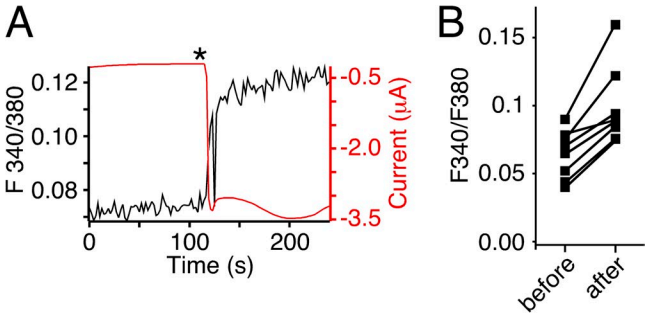

Figure 5. Activation of HyNaC increases $[Ca^{2+}]_i$ in oocytes. (A) Representative trace (black) from photometric Ca^{2+} measurements illustrating the increase of the F340/380 ratio in a HyNaC2/3/5-expressing oocyte after the application of RFamide I (asterisk). Oocytes had been injected with 50 nl Fura-2AM (1 mM) 30–120 min before the recording. Thus, the increased F340/380 ratio reflects an increase in $[Ca^{2+}]_i$. The red trace represents the current that paralleled the rise in $[Ca^{2+}]_i$. HyNaC was activated by pipetting Hydra-RFamide I into the bath to yield a final concentration of ~1 µM RFamide I. (B) Changes of the F340/F380 ratio caused by activation of HyNaC for individual measurements (n = 8).

shifted to 14 ± 2.5 mV (n = 8; Fig. 6 A), allowing us to calculate a permeability ratio P_{Ca}/P_{Na} = 3.85 (n = 8; see Materials and methods), which is in good agreement with a P_{Ca}/P_{mono} of P2X4.

We also calculated the permeability ratio P_{Na}/P_K of HyNaC by determining E_{rev} with 140 mM of either Na^+ or K^+, yielding a relative permeability P_{Na}/P_K = 3.0 (n = 8; not depicted), which is in agreement with previous results (Dürrnagel et al., 2010). The higher relative permeability for Na^+ over K^+ of HyNaC compared with P2X4 (P_{Na}/P_K of ∼1; Soto et al., 1996) can explain the slightly more positive E_{rev} of HyNaC in 10 mM Ca^{2+} (−17 ± 2.6 mV compared with −27 ± 1 mV; P < 0.01) in the experiment shown in Fig. 6 B.

In summary, we obtained consistent evidence for a high relative Ca^{2+} permeability of HyNaC.

Negative charges at the outer entrance to the ion pore are necessary for the high Ca^{2+} permeability of HyNaC

ASIC1a is a DEG/ENaC that is slightly permeable for Ca^{2+} (Waldmann et al., 1997; Bässler et al., 2001; Samways et al., 2009) and at the same time blocked by Ca^{2+} (Paukert et al., 2004). A ring of conserved aspartates at the outer mouth of the ASIC1a pore is crucial for Ca^{2+} block, presumably by constituting a Ca^{2+}-binding site (Paukert et al., 2004). These aspartates are conserved in HyNaC subunits 2, 3, and 5 (Fig. 7 A). Therefore we asked whether they contribute to Ca^{2+} permeability of HyNaCs. Substitution of the conserved aspartate by cysteine in all three HyNaC subunits (2/3/5; see Materials and methods) resulted in functional channels (HyNaC_D-C). Activation of HyNaC_D-C in oocytes evoked currents similar to HyNaC wild type (wt) (Fig. 7 B), but the presence of a peak current component was more variable, suggesting reduced activation of CaCCs by HyNaC_D-C. Furthermore, current amplitudes were smaller than those for HyNaC wt, as would be expected when CaCCs were less efficiently activated. To compensate for the smaller current amplitudes, we injected a 20-fold greater amount of cRNA for HyNaC_D-C. When we replaced Na^+ by $NMDG^+$ (keeping 1 mM Ca^{2+}) to abolish most of HyNaC_D-C inward currents, Hydra-RFamide I no longer elicited robust currents (Fig. 7 C), whereas it elicited robust inward currents in standard bath (I = 1 ± 0.25 µA; n = 5; Fig. 7 C). As we have shown above that the currents in the absence of Na^+ are CaCC currents, these findings indicate that activation of HyNaC_D-C did indeed not efficiently activate CaCCs and support reduced Ca^{2+} influx through HyNaC_D-C. In standard bath, E_{rev} of HyNaC_D-C was +16 ± 2 mV (n = 6; Fig. 7 D), indicative of a relatively unselective cation current, similar to HyNaC wt. Of note, HyNaC_D-C currents were not inwardly rectifying (Fig. 7 D), showing that the conserved Asp is necessary for inward rectification and in line with the requirement of Ca^{2+} for inward rectification. In EGTA-injected oocytes, HyNaC_D-C currents in the presence of 10 mM Ca^{2+} as the sole extracellular cation were tiny and approximately sevenfold smaller than in the presence of 10 mM Na^+ (0.01 ± 0.004 µA compared with 0.07 ± 0.01 µA; n = 11; Fig. 7 E); the addition of 10 mM Ca^{2+} to the Na^+-containing solution only slightly decreased the current amplitude by 29 ± 3% (0.05 ± 0.01 µA; n = 11; P < 0.001; Fig. 7 E), whereas for HyNaC wt, it decreased the current amplitude by 74 ± 2% (P < 0.001; Fig. 3 B). These results are consistent with the interpretation that HyNaC_D-C had a lower Ca^{2+} permeability and was less blocked by Ca^{2+} than HyNaC wt.

With 1 and 10 mM Ca^{2+} in EGTA-injected oocytes, the E_{rev} of HyNaC_D-C was significantly shifted to more negative potentials compared with HyNaC wt (n = 7–8; P < 0.001; Fig. 7, F and G), confirming a reduced Ca^{2+} permeability of HyNaC_D-C. The relative Ca^{2+} permeability of HyNaC_D-C, calculated by determining the shift in E_{rev} when the solution contained either Ca^{2+} or Na^+ as the main permeant cation (Fig. 7 F; see Materials and methods), was P_{Ca}/P_{Na} = 0.44 (n = 8), thus ninefold smaller than for HyNaC wt. In contrast, the permeability ratio for monovalent cations was comparable to HyNaC wt (P_{Na}/P_K = 2.9; n = 8; not depicted). These results suggest that the inefficient activation of CaCCs by HyNaC_D-C is caused by its strongly reduced Ca^{2+} permeability.

In photometric Ca^{2+} measurements, activation of HyNaC_D-C did not significantly increase the F340/F380 ratio (n = 8; P = 0.12; paired t test, Fig. 7 I; example in Fig. 7 H), consistent with a reduced Ca^{2+} influx in HyNaC_D-C–expressing oocytes. As expected, the

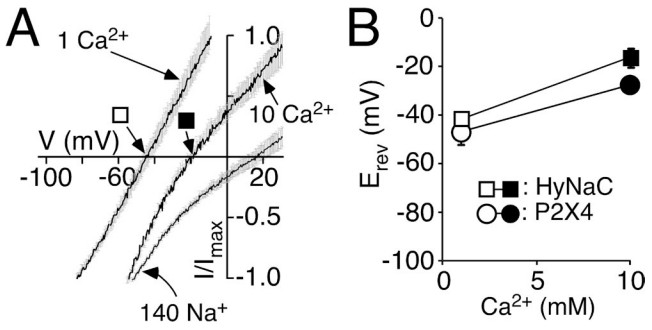

Figure 6. Permeability ratio P_{Ca}/P_{Na} of HyNaC is comparable to P2X4. (A) I/V relations of HyNaC2/3/5 in solutions containing 1 or 10 mM $CaCl_2$ and no NaCl (which had been replaced by 140 or 126.5 mM NMDG-Cl, respectively) and in a solution containing 140 mM NaCl and 1 mM $CaCl_2$. Continuous voltage ramps were run with a speed of 0.46 ms per millivolt (thus, for example, 6 s per 130 mV). Different voltage ranges were chosen for different conditions. Currents were normalized to I_{max}. Lines are the sum of 8–10 individual measurements. SEM is indicated by gray errors bars. 50 nl EGTA (20 mM) was injected before the recordings. Squares represent the E_{rev}s that are plotted in B. HyNaC was activated by 2 µM RFamide I. (B) Ca^{2+}-dependent shifts of the E_{rev} reveal a high Ca^{2+} permeability of HyNaC. E_{rev}s of the highly Ca^{2+}-permeable P2X4 receptor are shown for comparison and were similar to HyNaC. P2X4 was activated by 10 µM ATP.

increase in the F340/F380 ratio correlated with the current amplitude and could be fitted reasonably well with a line (Fig. 7 J). This linear regression analysis for the F340/F380 ratio change versus current showed a shallower slope for the D-C mutant than for HyNaC wt ($P < 0.01$; Fig. 7 J), which is also consistent with a reduced Ca^{2+} permeability of HyNaC_D-C.

DISCUSSION

HyNaCs are highly Ca^{2+} permeable

In a previous study (Dürrnagel et al., 2010), we described biphasic currents after the application of Hydra-RFamides in oocytes expressing HyNaC and entirely attributed these currents to currents flowing through the HyNaC pore. We concluded that HyNaC partially desensitizes and shows a tachyphylaxis from first to second peptide application. Moreover, we noted a variable ratio between transient and sustained currents (Dürrnagel et al., 2010).

Our new results show that those previous conclusions were wrong. HyNaCs are highly Ca^{2+}-permeable members of the DEG/ENaC gene family. In *Xenopus* oocytes, this high Ca^{2+} permeability leads to robust activation of the endogenous CaCC, and the Cl^- current adds to the cation current flowing through HyNaC itself. This secondary activation of the CaCC is entirely responsible for the biphasic appearance of peptide-activated

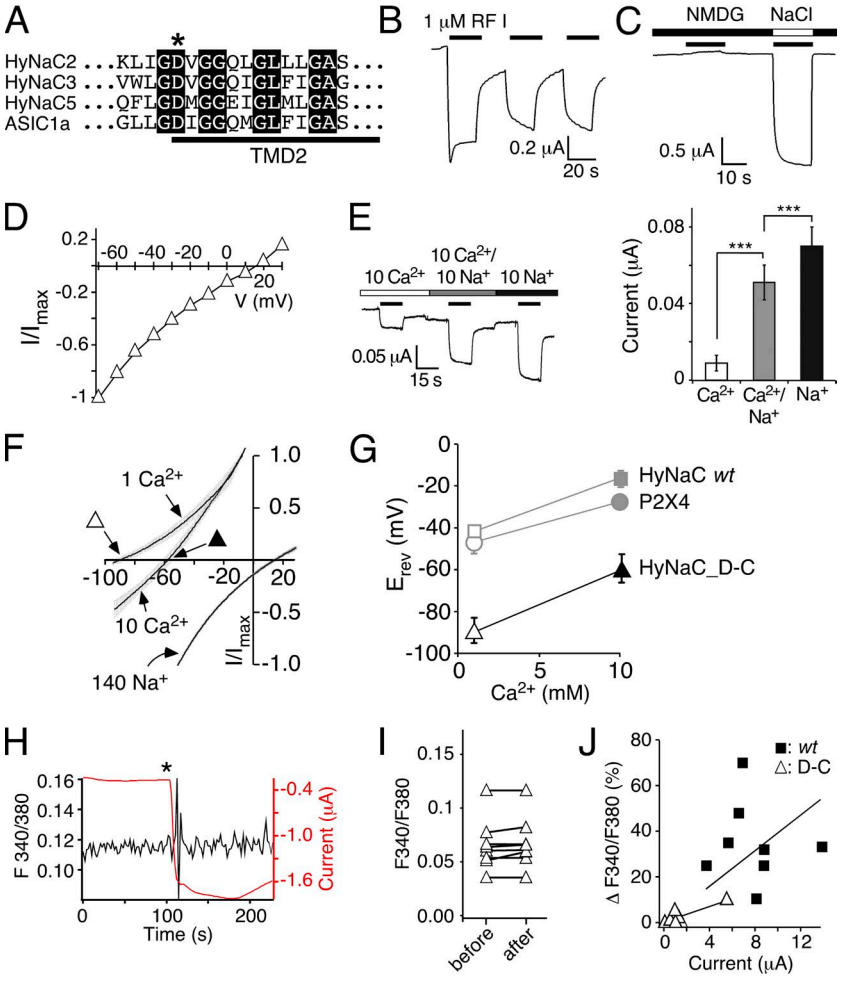

Figure 7. A conserved aspartate is necessary for the high Ca^{2+} permeability of HyNaC. (A) Alignment of the amino acid sequences of HyNaC2, 3, and 5 and ASIC1a at the beginning of the second transmembrane domain (TMD2) in the one-letter code. The crucial aspartate is indicated by an asterisk. Completely conserved amino acids are shown as white letters on a black background. (B) Representative current trace for HyNaC_D-C activated by 1 μM RFamide I. The amplitude and shape of the transient current component were more variable than for the wt. Mean maximum current amplitudes were 3.45 ± 1.2 μA for the first activation ($n = 5$). (C) Representative current trace showing activation of HyNaC_D-C by 1 μM RFamide I in solutions containing 1 mM Ca^{2+} together with either 140 mM $NMDG^+$ or Na^+. No inward current was visible in $NMDG^+$ solutions. (D) I/V plot for HyNaC_D-C activated by 1 μM RFamide I in standard bath solution. Currents were normalized to the current measured at −70 mV, which had an amplitude of −1.1 ± 0.2 μA ($n = 6$). (E; left) Representative current trace for HyNaC_D-C in solutions containing 10 mM Ca^{2+}, 10 mM Ca^{2+} and 10 mM Na^+, or 10 mM Na^+ (nominally free of Ca^{2+}). Conditions were as in Fig. 3 B. (Right) Quantitative comparison of current amplitudes. ***, $P < 0.001$. (F) I/V relations of HyNaC_D-C in solutions containing 1 or 10 mM $CaCl_2$ and no NaCl (which had been replaced by 140 or 126.5 mM NMDG-Cl, respectively) and in a solution containing 140 mM NaCl and 1 mM $CaCl_2$. Lines are the sum of eight to nine individual measurements. SEM is indicated by gray errors bars. Experimental conditions were as in Fig. 6 A. Triangles represent the E_{rev}s that are plotted in G. (G) Ca^{2+}-dependent shifts of the E_{rev} reveal a significantly lower Ca^{2+} permeability of HyNaC_D-C compared with HyNaC wt. E_{rev}s of HyNaC wt and P2X4 (gray symbols) are from Fig. 6 B and shown for comparison. (H) Representative trace (black) from photometric Ca^{2+} measurements illustrating no change of the F340/380 ratio after the application of ∼1 μM RFamide I (asterisk) in a oocyte expressing HyNaC_D-C. The deflections in the F340/380 ratio immediately after the peptide was added are caused by movements of the solution and are unspecific. Oocytes had been injected with 50 nl Fura-2AM (1 mM) 30–120 min before the recording. The red trace represents the current that robustly increased after peptide application. (I) F340/F380 before and after the application of ∼1 μM RFamide I for HyNaC_D-C ($n = 8$). (J) Plot of the increase of the F340/380 ratio (as percentage) after the application of RFamide I as a function of peptide-activated current amplitudes. Closed squares represent individual measurements for HyNaC wt, and open triangles are for HyNaC_D-C ($n = 8$). Current amplitudes were smaller for HyNaC_D-C than for HyNaC wt ($n = 8$; $P < 0.001$; Fig. 5 B). Solid lines represent linear fits of the fluorescence/current ratio. Note that the slope of this line was larger for wt than for the D-C mutant, indicating a higher relative Ca^{2+} permeability of the wt.

currents in HyNaC-expressing oocytes. This conclusion is based on several different observations: (a) E_{rev} of the transient current is Cl^- dependent; (b) intracellular chelation of Ca^{2+} abolishes the transient current and leads to step-like HyNaC currents; (c) Hydra-RFamides elicit biphasic inward currents also in the absence of permeant monovalent cations; (d) Ca^{2+} measurements reveal an increase in $[Ca^{2+}]_i$ that parallels the opening of the HyNaC pore; and (e) E_{rev} of HyNaC is Ca^{2+} dependent. These results consistently show that HyNaCs are Ca^{2+} permeable. Moreover, our results show that HyNaC currents have no strong time dependence; in the presence of the intracellular Ca^{2+} chelators EGTA or BAPTA, Hydra-RFamides elicit step-like currents that do not desensitize. The apparent biphasic HyNaC current and tachyphylaxis from first to second peptide application (Golubovic et al., 2007; Dürrnagel et al., 2010) arise from the secondary activation of the CaCC. Consequently, tachyphylaxis was abolished in cells injected with EGTA (Fig. 2 A).

Several ligand-gated channels share a high Ca^{2+} permeability with HyNaCs and activate CaCCs when expressed in *Xenopus* oocytes, among them NMDA receptors (Leonard and Kelso, 1990), kainate receptor GluR6 (Egebjerg and Heinemann, 1993), α_7 and α_9 nicotinic acetylcholine receptors (Galzi et al., 1992; Vernino et al., 1992; Séguéla et al., 1993; Katz et al., 2000), and purinergic P2X4 receptors (Soto et al., 1996). Our estimates of the Ca^{2+} permeability of HyNaCs, P_{Ca}/P_{Na} = 3.85, revealed a Ca^{2+} permeability similar to that of P2X4 (Soto et al., 1996), P_{Ca}/P_{mono} = 4.2, placing HyNaCs among the highly Ca^{2+}-permeable ligand-gated ion channels. We note, however, that P_{Ca}/P_{Na} ratios obtained by measurements of the shift in E_{rev}s generally have to be regarded with caution, as the Goldman–Hodgkin–Katz constant field voltage equation, which was used to calculate permeability ratios, requires that there is no interaction among permeating ions (Burnashev et al., 1995; Hille, 2001). Like for most ion channels, this is not the case for HyNaCs, implying that P_{Ca}/P_{Na} is not constant but depends in a complex manner on the voltage and the individual concentrations of divalent and monovalent ions on both sides of the membrane. For example, for HyNaC we estimated a ratio of $P_{Ca}/P_{Na} \approx 10$, when using E_{rev} in a solution containing 1 mM (instead of 10 mM) Ca^{2+}.

The FMRFamide-activated Na^+ channel, FaNaC, is another peptide-gated ion channel from the DEG/ENaC gene family (Lingueglia et al., 1995). When expressed in oocytes, FMRFamide elicits currents that develop comparatively slowly over a few seconds and that partially desensitize. Moreover, FaNaC shows an E_{rev} indicative of a highly Na^+-selective ion channel (Lingueglia et al., 1995). Thus, kinetics and ion selectivity are considerably different between the only two known peptide-gated ion channels, both from the DEG/ENaC gene family.

A conserved Asp confers high Ca^{2+} permeability

In addition, we show that a conserved aspartate is necessary for the high Ca^{2+} permeability of HyNaCs. Again, several observations support this conclusion: (a) when the conserved aspartate was substituted by a cysteine (HyNaC_D-C), Hydra-RFamides elicit no strong inward currents in the absence of permeant monovalent cations; (b) E_{rev} with Ca^{2+} as main charge carrier was significantly shifted compared with wt; (c) the relative Ca^{2+} permeability was reduced to P_{Ca}/P_{Na} = 0.44; and (d) photometric Ca^{2+} measurements revealed no increase in $[Ca^{2+}]_i$ when channels opened. The aspartate is conserved in ASICs and is crucial for Ca^{2+} block of ASICs (Paukert et al., 2004) and for coordinating monovalent cations at the outer ASIC pore (Gonzales et al., 2009). Thus, it is likely that these aspartates form a ring of negative charges at the outer entry of the HyNaC pore that attracts cations, in particular Ca^{2+}. Removing the aspartate abolished inward rectification, suggesting that the aspartate is a determinant of a Ca^{2+}-binding site, which mediates Ca^{2+} block and thus inward rectification of HyNaC.

Because ASICs also have the crucial Asp but are impermeable for Ca^{2+}, with the exception of ASIC1a that has a low Ca^{2+} permeability (Bässler et al., 2001;

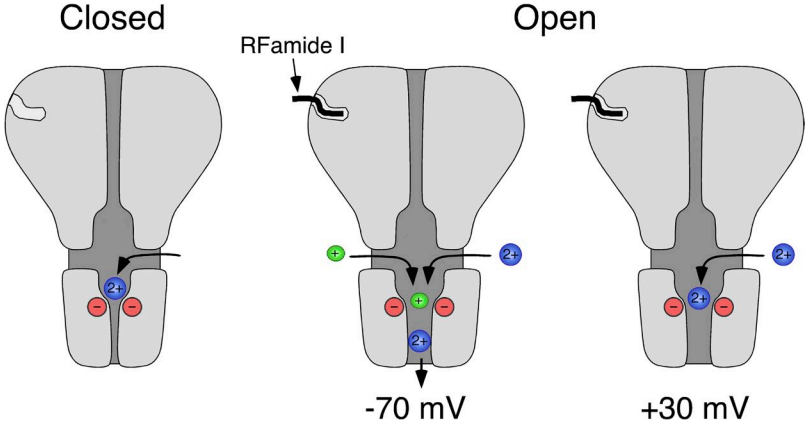

Figure 8. Scheme illustrating Ca^{2+} permeation through HyNaC. In the closed conformation (left), Ca^{2+} can probably access the extracellular vestibule through three lateral fenestrations (Jasti et al., 2007; Li et al., 2011) and bind to the conserved aspartates at the outer mouth of the ion pore. After binding of the ligand, HyNaC opens and, at negative membrane potentials, Ca^{2+} permeates the channel (−70 mV, middle), liberating the ion pore. At depolarized potentials (+30 mV, right), however, Ca^{2+} remains bound to the ring of negative charges and blocks the open pore. Based on the crystal structure of chicken ASIC1 (Jasti et al., 2007).

Samways et al., 2009), the Asp is necessary but not sufficient for Ca^{2+} permeability of HyNaCs. Reminiscent of this situation, for NMDA receptor channels it has been proposed that Ca^{2+} interacts with "external" and "deep" sites, corresponding to regions at the external mouth and central in the pore of the channel, respectively (Watanabe et al., 2002). The conserved aspartate of HyNaCs and ASICs could represent an external Ca^{2+}-interaction site, and the putative internal site would also be necessary for Ca^{2+} permeation. In fact, for ASIC1, amino acids at the intracellular N terminus determine Ca^{2+} permeability (Bässler et al., 2001). Future experiments will show whether the high Ca^{2+} permeability of HyNaCs also depends on their intracellular N termini or other regions along the axis of their pore.

Collectively, our results suggest the following scenario (Fig. 8). Ca^{2+} gets attracted to the outer mouth of the HyNaC pore by the negative charges of the conserved ring of aspartates. At positives potentials (for example, +30 mV), Ca^{2+} inefficiently permeates the channel and blocks the open pore, presumably by tightly binding to the aspartates. At more negative potentials (for example, −70 mV) Ca^{2+} more efficiently permeates the channel, liberating the pore for the passage also of monovalent cations.

HyNaCs are the first DEG/ENaCs with a high Ca^{2+} permeability

So far, all DEG/ENaCs have been found to be more or less Na^+ selective; in fact, Na^+ selectivity is a defining hallmark of these channels. In the few exceptions, where DEG/ENaCs are associated with unselective ion pores, the unselective state coexists with a Na^+-selective state, as in the case of some ASICs (Lingueglia et al., 1997; Springauf and Gründer, 2010) and rat brain liver intestine Na^+ channel (rBLINaC, now named bile acid–sensitive ion channel, or BASIC) (Sakai et al., 1999; Wiemuth and Gründer, 2010; Wiemuth et al., 2012). In these cases, the Na^+-selective state probably carries most of the current under physiological conditions. MEC-4, a subunit of a mechanosensitive DEG/ENaC from *C. elegans* (Driscoll and Chalfie, 1991), can be constitutively activated by mutation (MEC-4(d)) and then carries a Ca^{2+} component with a permeability ratio of Ca^{2+} versus Na^+ (P_{Ca}/P_{Na}) of 0.22 (Bianchi et al., 2004), >10 times lower than for HyNaCs. Moreover, the physiologically relevant current carried by Mec-4 is a Na^+ current (Goodman et al., 2002; O'Hagan et al., 2005). Thus, HyNaCs are the first DEG/ENaCs that are unselective cation channels with a high Ca^{2+} permeability.

At present, we can only speculate on the role of Ca^{2+} permeability for the physiological function of HyNaCs. HyNaCs are expressed at the base of the tentacles, perhaps in epitheliomuscular cells, and the preprohormone gene that encodes their ligands (Darmer et al., 1998), Hydra-RFamides I and II, is expressed in adjacent nerve cells of the hypostome and upper gastric region (Hansen et al., 2000). Therefore, it has been speculated that HyNaCs contribute to coordinate the *Hydra* feeding response (Golubovic et al., 2007; Dürrnagel et al., 2010). In agreement with this hypothesis, Antho-RFamide (pQGRF-NH_2), a related RFamide peptide from anthozoans, another class within the phylum Cnidaria that contains sea anemones, has excitatory actions on sea anemone muscle preparations and increases the frequency of spontaneous tentacle contractions (McFarlane et al., 1991). Thus, the action of Antho-RFamide is compatible with the idea that Hydra-RFamides are transmitters at neuromuscular junctions and that HyNaCs are their postsynaptic receptors. Of note, another anthozoan neuropeptide, Antho-RWamide I (pQSLRW-NH_2), increases an inward Ca^{2+} current in endodermal myoepithelial cells of sea anemones (Cho and McFarlane, 1996). Whatever the exact physiological function of HyNaCs is, it is likely that Ca^{2+} influx through open HyNaCs supports their function. The block by Ca^{2+} of HyNaC will limit influx of Ca^{2+}, especially at more depolarized membrane potentials.

In summary, we show that HyNaC has simple kinetics and does not desensitize in the prolonged presence of its ligands, and that HyNaC is an unselective cation channel with a high Ca^{2+} permeability, which is an uncommon feature of DEG/ENaCs. Therefore, it is possible that the highly selective Na^+ pore of DEG/ENaCs that is a characterizing feature of these channels is in fact a feature that was not shared by the common ancestor and developed during evolution.

This work was supported by the Deutsche Forschungsgemeinschaft (grant GR 1771/7-1 to S. Gründer) and the Interdisciplinary Centre for Clinical Research within the Faculty of Medicine at RWTH Aachen University (grant N5-1 to B.H. Falkenburger).

Lawrence G. Palmer served as editor.

Submitted: 13 March 2012
Accepted: 4 September 2012

REFERENCES

Barish, M.E. 1983. A transient calcium-dependent chloride current in the immature Xenopus oocyte. *J. Physiol.* 342:309–325.

Bässler, E.L., T.J. Ngo-Anh, H.S. Geisler, J.P. Ruppersberg, and S. Gründer. 2001. Molecular and functional characterization of acid-sensing ion channel (ASIC) 1b. *J. Biol. Chem.* 276:33782–33787. http://dx.doi.org/10.1074/jbc.M104030200

Bianchi, L., B. Gerstbrein, C. Frøkjaer-Jensen, D.C. Royal, G. Mukherjee, M.A. Royal, J. Xue, W.R. Schafer, and M. Driscoll. 2004. The neurotoxic MEC-4(d) DEG/ENaC sodium channel conducts calcium: implications for necrosis initiation. *Nat. Neurosci.* 7:1337–1344. http://dx.doi.org/10.1038/nn1347

Boton, R., D. Singer, and N. Dascal. 1990. Inactivation of calcium-activated chloride conductance in Xenopus oocytes: roles of calcium and protein kinase C. *Pflugers Arch.* 416:1–6. http://dx.doi.org/10.1007/BF00370214

Burnashev, N., Z. Zhou, E. Neher, and B. Sakmann. 1995. Fractional calcium currents through recombinant GluR channels of the

NMDA, AMPA and kainate receptor subtypes. *J. Physiol.* 485: 403–418.

Cho, K., and I.D. McFarlane. 1996. The anthozoan neuropeptide Antho-RWamide I modulates Ca2+ current in sea anemone myoepithelial cells. *Neurosci. Lett.* 209:53–56. http://dx.doi.org/10.1016/0304-3940(96)12597-0

Cottrell, G.A., K.A. Green, and N.W. Davies. 1990. The neuropeptide Phe-Met-Arg-Phe-NH2 (FMRFamide) can activate a ligand-gated ion channel in Helix neurones. *Pflugers Arch.* 416:612–614. http://dx.doi.org/10.1007/BF00382698

Darmer, D., F. Hauser, H.P. Nothacker, T.C. Bosch, M. Williamson, and C.J.P. Grimmelikhuijzen. 1998. Three different prohormones yield a variety of Hydra-RFamide (Arg-Phe-NH2) neuropeptides in Hydra magnipapillata. *Biochem. J.* 332:403–412.

Davies, C.W. 1962. Ion Association. Butterworths, London. 190 pp.

Driscoll, M., and M. Chalfie. 1991. The mec-4 gene is a member of a family of Caenorhabditis elegans genes that can mutate to induce neuronal degeneration. *Nature.* 349:588–593. http://dx.doi.org/10.1038/349588a0

Dürrnagel, S., A. Kuhn, C.D. Tsiairis, M. Williamson, H. Kalbacher, C.J. Grimmelikhuijzen, T.W. Holstein, and S. Gründer. 2010. Three homologous subunits form a high affinity peptide-gated ion channel in Hydra. *J. Biol. Chem.* 285:11958–11965. http://dx.doi.org/10.1074/jbc.M109.059998

Egebjerg, J., and S.F. Heinemann. 1993. Ca2+ permeability of unedited and edited versions of the kainate selective glutamate receptor GluR6. *Proc. Natl. Acad. Sci. USA.* 90:755–759. http://dx.doi.org/10.1073/pnas.90.2.755

Galzi, J.L., A. Devillers-Thiéry, N. Hussy, S. Bertrand, J.P. Changeux, and D. Bertrand. 1992. Mutations in the channel domain of a neuronal nicotinic receptor convert ion selectivity from cationic to anionic. *Nature.* 359:500–505. http://dx.doi.org/10.1038/359500a0

Golubovic, A., A. Kuhn, M. Williamson, H. Kalbacher, T.W. Holstein, C.J. Grimmelikhuijzen, and S. Gründer. 2007. A peptide-gated ion channel from the freshwater polyp Hydra. *J. Biol. Chem.* 282:35098–35103. http://dx.doi.org/10.1074/jbc.M706849200

Gonzales, E.B., T. Kawate, and E. Gouaux. 2009. Pore architecture and ion sites in acid-sensing ion channels and P2X receptors. *Nature.* 460:599–604. http://dx.doi.org/10.1038/nature08218

Goodman, M.B., G.G. Ernstrom, D.S. Chelur, R. O'Hagan, C.A. Yao, and M. Chalfie. 2002. MEC-2 regulates C. elegans DEG/ENaC channels needed for mechanosensation. *Nature.* 415:1039–1042. http://dx.doi.org/10.1038/4151039a

Hansen, G.N., M. Williamson, and C.J.P. Grimmelikhuijzen. 2000. Two-color double-labeling in situ hybridization of whole-mount Hydra using RNA probes for five different Hydra neuropeptide preprohormones: evidence for colocalization. *Cell Tissue Res.* 301:245–253. http://dx.doi.org/10.1007/s004410000240

Hille, B. 2001. Ion Channels of Excitable Membranes. Third edition. Sinauer Associates, MA. 814 pp.

Jasti, J., H. Furukawa, E.B. Gonzales, and E. Gouaux. 2007. Structure of acid-sensing ion channel 1 at 1.9 Å resolution and low pH. *Nature.* 449:316–323. http://dx.doi.org/10.1038/nature06163

Katz, E., M. Verbitsky, C.V. Rothlin, D.E. Vetter, S.F. Heinemann, and A.B. Elgoyhen. 2000. High calcium permeability and calcium block of the alpha9 nicotinic acetylcholine receptor. *Hear. Res.* 141:117–128. http://dx.doi.org/10.1016/S0378-5955(99)00214-2

Kellenberger, S., and L. Schild. 2002. Epithelial sodium channel/degenerin family of ion channels: a variety of functions for a shared structure. *Physiol. Rev.* 82:735–767.

Leonard, J.P., and S.R. Kelso. 1990. Apparent desensitization of NMDA responses in Xenopus oocytes involves calcium-dependent chloride current. *Neuron.* 4:53–60. http://dx.doi.org/10.1016/0896-6273(90)90443-J

Lewis, C.A. 1979. Ion-concentration dependence of the reversal potential and the single channel conductance of ion channels at the frog neuromuscular junction. *J. Physiol.* 286:417–445.

Li, T., Y. Yang, and C.M. Canessa. 2011. Outlines of the pore in open and closed conformations describe the gating mechanism of ASIC1. *Nat Commun.* 2:399. http://dx.doi.org/10.1038/ncomms1409

Lingueglia, E., G. Champigny, M. Lazdunski, and P. Barbry. 1995. Cloning of the amiloride-sensitive FMRFamide peptide-gated sodium channel. *Nature.* 378:730–733. http://dx.doi.org/10.1038/378730a0

Lingueglia, E., J.R. de Weille, F. Bassilana, C. Heurteaux, H. Sakai, R. Waldmann, and M. Lazdunski. 1997. A modulatory subunit of acid sensing ion channels in brain and dorsal root ganglion cells. *J. Biol. Chem.* 272:29778–29783. http://dx.doi.org/10.1074/jbc.272.47.29778

Madeja, M., U. Musshoff, and E.J. Speckmann. 1995. Improvement and testing of a concentration-clamp system for oocytes of Xenopus laevis. *J. Neurosci. Methods.* 63:211–213. http://dx.doi.org/10.1016/0165-0270(95)00094-1

McFarlane, I.D., P.A. Anderson, and C.J. Grimmelikhuijzen. 1991. Effects of three anthozoan neuropeptides, Antho-RWamide I, Antho-RWamide II and Antho-RFamide, on slow muscles from sea anemones. *J. Exp. Biol.* 156:419–431.

Miledi, R. 1982. A calcium-dependent transient outward current in Xenopus laevis oocytes. *Proc. R. Soc. Lond. B Biol. Sci.* 215:491–497. http://dx.doi.org/10.1098/rspb.1982.0056

Moosler, A., K.L. Rinehart, and C.J.P. Grimmelikhuijzen. 1996. Isolation of four novel neuropeptides, the hydra-RFamides I-IV, from Hydra magnipapillata. *Biochem. Biophys. Res. Commun.* 229: 596–602. http://dx.doi.org/10.1006/bbrc.1996.1849

O'Hagan, R., M. Chalfie, and M.B. Goodman. 2005. The MEC-4 DEG/ENaC channel of Caenorhabditis elegans touch receptor neurons transduces mechanical signals. *Nat. Neurosci.* 8:43–50. http://dx.doi.org/10.1038/nn1362

Paukert, M., E. Babini, M. Pusch, and S. Gründer. 2004. Identification of the Ca^{2+} blocking site of acid-sensing ion channel (ASIC) 1: Implications for channel gating. *J. Gen. Physiol.* 124:383–394. http://dx.doi.org/10.1085/jgp.200308973

Sakai, H., E. Lingueglia, G. Champigny, M.G. Mattei, and M. Lazdunski. 1999. Cloning and functional expression of a novel degenerin-like Na+ channel gene in mammals. *J. Physiol.* 519:323–333. http://dx.doi.org/10.1111/j.1469-7793.1999.0323m.x

Samways, D.S., A.B. Harkins, and T.M. Egan. 2009. Native and recombinant ASIC1a receptors conduct negligible Ca2+ entry. *Cell Calcium.* 45:319–325. http://dx.doi.org/10.1016/j.ceca.2008.12.002

Schroeder, B.C., T. Cheng, Y.N. Jan, and L.Y. Jan. 2008. Expression cloning of TMEM16A as a calcium-activated chloride channel subunit. *Cell.* 134:1019–1029. http://dx.doi.org/10.1016/j.cell.2008.09.003

Séguéla, P., J. Wadiche, K. Dineley-Miller, J.A. Dani, and J.W. Patrick. 1993. Molecular cloning, functional properties, and distribution of rat brain alpha 7: a nicotinic cation channel highly permeable to calcium. *J. Neurosci.* 13:596–604.

Soto, F., M. Garcia-Guzman, J.M. Gomez-Hernandez, M. Hollmann, C. Karschin, and W. Stühmer. 1996. P2X4: an ATP-activated ionotropic receptor cloned from rat brain. *Proc. Natl. Acad. Sci. USA.* 93:3684–3688. http://dx.doi.org/10.1073/pnas.93.8.3684

Springauf, A., and S. Gründer. 2010. An acid-sensing ion channel from shark (Squalus acanthias) mediates transient and sustained responses to protons. *J. Physiol.* 588:809–820. http://dx.doi.org/10.1113/jphysiol.2009.182931

Vernino, S., M. Amador, C.W. Luetje, J. Patrick, and J.A. Dani. 1992. Calcium modulation and high calcium permeability of neuronal nicotinic acetylcholine receptors. *Neuron.* 8:127–134. http://dx.doi.org/10.1016/0896-6273(92)90114-S

Waldmann, R., G. Champigny, F. Bassilana, C. Heurteaux, and M. Lazdunski. 1997. A proton-gated cation channel involved in acid-sensing. *Nature.* 386:173–177. http://dx.doi.org/10.1038/386173a0

Watanabe, J., C. Beck, T. Kuner, L.S. Premkumar, and L.P. Wollmuth. 2002. DRPEER: a motif in the extracellular vestibule conferring high Ca2+ flux rates in NMDA receptor channels. *J. Neurosci.* 22:10209–10216.

White, M.M., and M. Aylwin. 1990. Niflumic and flufenamic acids are potent reversible blockers of Ca2(+)-activated Cl- channels in Xenopus oocytes. *Mol. Pharmacol.* 37:720–724.

Wiemuth, D., and S. Gründer. 2010. A single amino acid tunes Ca2+ inhibition of brain liver intestine Na+ channel (BLINaC). *J. Biol. Chem.* 285:30404–30410. http://dx.doi.org/10.1074/jbc.M110.153064

Wiemuth, D., H. Sahin, B.H. Falkenburger, C.M. Lefèvre, H.E. Wasmuth, and S. Gründer. 2012. BASIC—a bile acid-sensitive ion channel highly expressed in bile ducts. *FASEB J.* In press.

Wu, G., and O.P. Hamill. 1992. NPPB block of Ca(++)-activated Cl- currents in Xenopus oocytes. *Pflugers Arch.* 420:227–229. http://dx.doi.org/10.1007/BF00374996